



A facile approach to fabricate Ni inverse opals at controlled thickness

Yi-Jui Huang, Chun-Han Lai, Pu-Wei Wu^{*}, Li-Yin Chen

Department of Materials Science and Engineering, National Chiao Tung University, Hsinchu 300, Taiwan, ROC

ARTICLE INFO

Article history:

Received 29 July 2009

Accepted 17 August 2009

Available online 23 August 2009

Keywords:

Electrophoretic deposition

Colloidal crystals

Ni plating

Inverse opals

ABSTRACT

A vertical electrophoretic deposition method was employed to fabricate polystyrene (PS) colloidal crystals with negligible defects and considerable surface uniformity. Subsequently, the interstitial voids within the colloidal crystals were electroplated with Ni, followed by selective removal of the PS microspheres. With careful adjustment in the processing parameters, we were able to obtain Ni inverse opals at predetermined thickness in relatively short time. The inverse opals revealed superb structural stability and surface uniformity. Because the electrophoresis and electrodeposition were both carried out in a solution state, this fabrication scheme enables facile construction of inverse opals on conductive substrates over conventional approaches.

© 2009 Elsevier B.V. All rights reserved.

1. Introduction

Assembly of monodisperse microspheres into three-dimensional colloidal crystals is of particular interest for potential applications in photonic crystals and biosensors [1,2]. So far, assembly approaches such as solvent evaporation, gravity sedimentation, spatial patterning, and electrophoresis have been explored with various successes [3–6]. Recently, it was demonstrated that by filling the interstitial voids within the colloidal crystals with metals, followed by selective removal of microspherical template, an inverse opal can be obtained [7,8]. Due to its periodic metal skeleton, the inverse structure revealed unique properties in thermal emission and magnetics [9,10].

Conventional methods to fill metals within the interstitial voids involve chemical conversion, chemical vapor deposition, and ionic spraying [11–13]. In addition to metals, oxides are successfully deposited as well [14,15]. However, those fabrication techniques typically require excessive processing time at moderate yield. Moreover, exact control in the thickness and surface uniformity is often lacking. In contrast, the electroplating route provides a simple and efficient metal deposition scheme [16].

To fabricate the Ni inverse opals at controlled thickness, it is necessary first to prepare the colloidal crystals in desirable forms. It is because structural arrangement of the colloidal crystals plays a critical role over subsequent electroplating process. In electroplating, the electrolyte path affects the iR loss that determines the area for accelerated deposition. Hence, to obtain the deposit with considerable height uniformity, a relatively consistent electrolyte path is necessary. To meet this criterion, a close-packed colloidal crystal with reduced defects and superb surface uniformity becomes essential. Only when both conditions are met, we could maintain the length for electrolyte

percolation over the entire colloidal crystals, leading to a steady Ni plating rate on every spot.

Previously, we conducted the electrophoresis of SiO_2 microspheres in a vertical arrangement and fabricated colloidal crystals with negligible defects and impressive surface uniformity [17]. In this work, we adopt a similar approach to prepare the PS colloidal crystals and demonstrate the construction of Ni inverse opals at various layers by deliberate control in relevant processing parameters.

2. Experimental

We synthesized the PS microspheres using an emulsifier-free emulsion polymerization process [18]. First, styrene was used as the monomer after removing inhibitors and $\text{K}_2\text{S}_2\text{O}_8$ was used as the initiator. The polymerization was performed at 70 °C and the resulting PS microspheres demonstrated an average diameter of 660 nm with a standard deviation of 16.4 nm. Assembly of PS microspheres was carried out by an electrophoretic deposition technique in a vertical arrangement at room temperature. First, the as-synthesized PS microspheres (0.5 g) were dispersed in a solution of ethanol (100 mL) and deionized water (100 mL). The pH for the mixture was adjusted to 10 to form a stable suspension. In subsequent electrophoretic depositions, a Si wafer (4 cm²) pre-sputtered with 500 nm of Ti as a conductive overcoat was employed as the substrate. A stainless plate (25 cm²) was used as the counter electrode. We adjusted the electrical field at 10 V/cm for 15 min to allow proper assembly of microspheres at sufficient thickness. Next, the colloidal crystals were removed and dried in air at 50 °C for 10 min.

To fabricate Ni inverse opals, a Ni plating bath consisting of $\text{NiSO}_4 \cdot 6\text{H}_2\text{O}$ (130 g/L), $\text{NiCl}_2 \cdot 6\text{H}_2\text{O}$ (30 g/L), and H_3BO_3 (18 g/L) was adopted. The PS colloidal crystals and Ni plate (25 cm²) were used as working and counter electrodes, respectively. Their distance was 2.5 cm. The electroplating was conducted at 1 V for 10–60 min. After those

^{*} Corresponding author. Tel.: +886 3 5131227; fax: +886 3 5724727.
E-mail address: ppwu@mail.nctu.edu.tw (P.-W. Wu).

interstitial voids were completely filled by the Ni, the PS microspheres were removed by immersing in an ethyl acetate (95 wt.%) solution for 24 h at 26 °C.

Scanning Electron Microscope (SEM; Joel JSM-6700F) was used to observe the morphologies for the colloidal crystals and inverse opals. Electrophoresis and electroplating were conducted by a BaSyTec instrument.

3. Results and discussion

To construct inverse opals with structural integrity and surface uniformity, it is necessary to fabricate colloidal crystals in appropriate thickness. It is because during electroplating, excess thickness might lead to undesirable height variation for the plated Ni. On the other hand, inadequate thickness resulted in unstable colloidal film that detached from the substrate during electroplating. After extensive tries, we selected 15 min of electrophoresis at 10 V/cm to prepare the colloidal crystals for subsequent Ni electroplating. Fig. 1 provides the SEM images in cross-sectional and top views for the PS colloidal crystals. As shown in Fig. 1(a), the sample surface was rather flat. This unique character is attributed to our vertical electrophoresis design that allows dense and close-packed microspheres. After 15 min of electrophoretic deposition, we obtained colloidal crystals at a height of 26.5 μm , which corresponds to 56 layers of PS microspheres. Fig. 1(b) displays the PS colloidal crystals in top view. A close-packed fcc (111) lattice was clearly visible. Some vacancies were also observed but they appeared on the surface layer only. Our previous experiences indicated very few vacancies were formed underneath.

Fig. 2 exhibits the current profile as a function of electroplating time. Apparently, the current rose initially for the first 30 min and stabilized with slow increment afterward. This behavior is consistent with what was reported earlier in similar experiments [19,20]. Since the Ni electrodeposition was performed at constant 1 V, the recorded current was inversely proportional to the sum of the electrolyte iR loss and Ni charge transfer resistance. Because the Ni reduction and

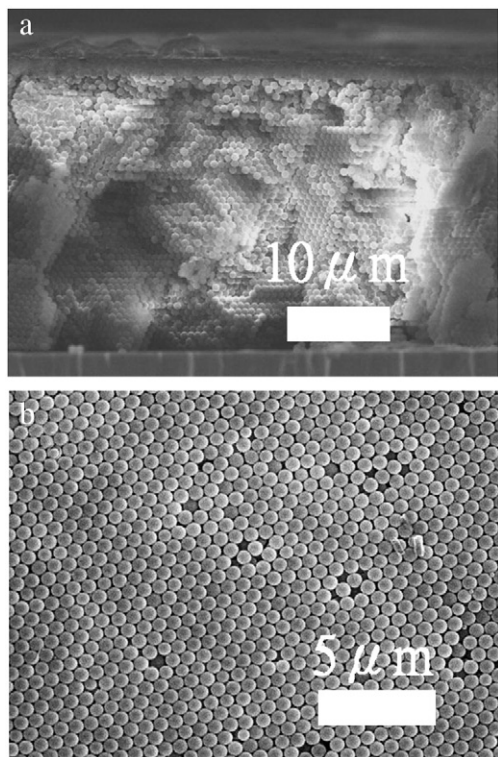


Fig. 1. SEM images for PS colloidal crystals in (a) cross-sectional and (b) top views.

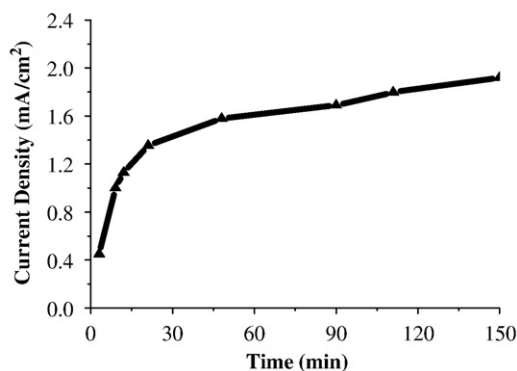


Fig. 2. Current density as a function of plating time during electroplating of PS colloidal crystals.

deposition were relatively simple, its charge transfer resistance was likely to remain unchanged. Hence, we believe that the changeup in the electrolyte iR loss was primarily responsible for the observed current variation. The predominant factor in the electrolyte iR loss was the electrolyte access distance. Electroplating was typically initiated at the bottom of colloidal crystals that represented the longest percolation length. With time progressed, electrolyte percolation became less difficult with shortened path that lead to the measured current increase.

SEM pictures for the Ni inverse opals in cross-sectional views undergoing electroplating of 10, 15, 20, and 30 min are demonstrated in Fig. 3. They corresponded to inverse opals with approximate layers of 1, 2, 3, and 7 layers, respectively. The insets are their respective top view images. Obviously, the Ni formed a continuous network occupying the interstitial voids among the PS microspheres. The inverse opals contained hexagonal arrays of pores left by the PS microspheres. The size for those pores was consistent with the diameter of the PS microspheres. Notably, the Ni inverse structure revealed impressive mechanical strength and structural integrity at different layers. Moreover, the Ni inverse opals exhibited impressive height consistency indicating the electroplating process took place at a similar rate everywhere. The ability to construct inverse opals at controlled thickness is rather appealing. It is because many physical and chemical properties of the inverse opals depend on their thickness. For example, Xia et al. reported that the photonic bandgap displayed considerable sensitivity to the thickness [21]. In addition, Eagleton and Searson determined the surface area of the inverse opals by thickness and studied the resulting magnetic responses correspondingly [19].

Excluding the PS template removal time, our fabrication scheme enables facile construction of inverse opals in multiple layers within 60 min. This is a substantially reduced processing time as opposed to conventional methods of more than 24 h [19,20]. Moreover, since both electrophoresis and electroplating were carried out in a solution state on the same substrate, interference from sample handling and transfer was largely reduced. As a result, structural integrity of the inverse opals was nicely maintained.

4. Conclusion

Ni inverse opals at controlled thickness were successfully demonstrated using a vertical electrophoretic deposition technique to prepare PS colloidal crystals first, followed by potentiostatic Ni electrodeposition and chemical removal of PS microspheres. Because the PS colloidal crystals revealed significantly reduced defects and considerable surface uniformity, we were able to electroplate Ni into those interstitial voids to reach predetermined thickness. Our fabrication scheme allows simple construction of inverse opals on conductive substrates in relatively short time.

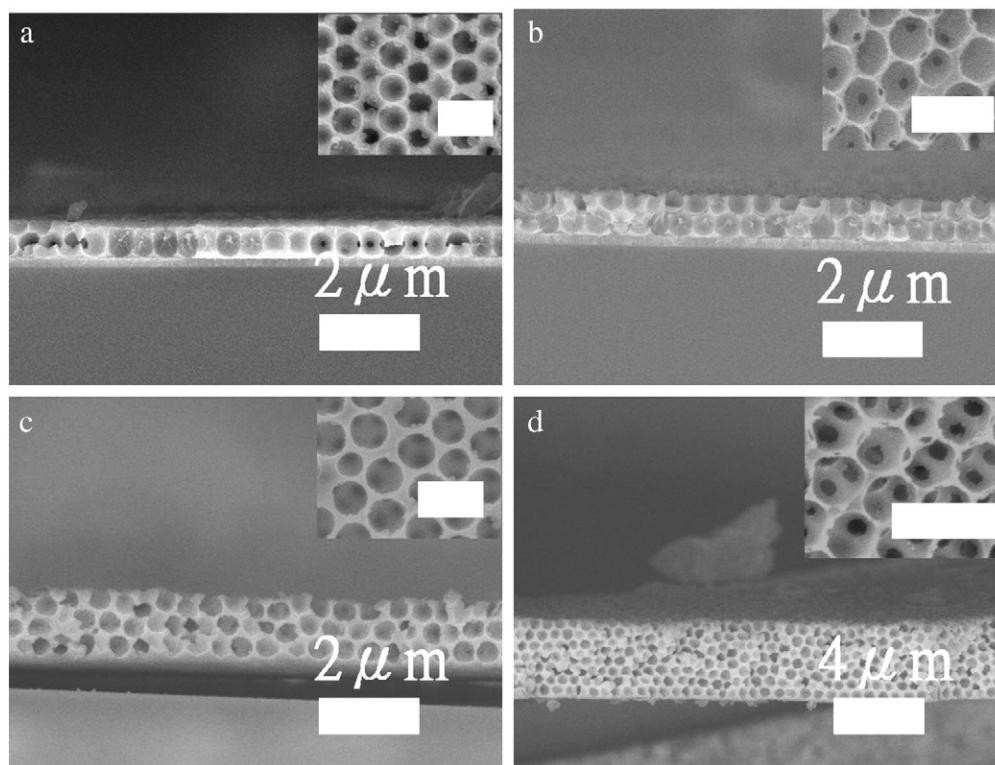


Fig. 3. Cross-sectional SEM images for Ni inverse opals in (a) 1, (b) 2, (c) 3, and (d) 7 layers, respectively. The insets are their respective top views with the scale bar in 1 μm .

Acknowledgements

Equipment loans from Professor Pang Lin and Professor George Tu are greatly appreciated.

References

- [1] Cho GJ, Jung MH, Yang HT, Lee BK, Song JH. *Mater Lett* 2007;61:1086–90.
- [2] Chen SH, Yuan R, Chai YQ, Xu L, Wang N, Li XN, et al. *Electroanalysis* 2006;18:471–7.
- [3] Hoogenboom JP, Rétif C, Bres E, Boer M, Langen-Suurling AK, Romijn J, et al. *Nano Lett* 2004;4:205–8.
- [4] Li QY, Chen YF, Dong P. *Mater Lett* 2005;59:3521–4.
- [5] Masuda Y, Itoh T, Itoh M, Koumoto K. *Langmuir* 2004;20:5588–92.
- [6] Choi WM, Park OO. *Nanotechnology* 2006;17:325–9.
- [7] Napolskii K, Sapoletova N, Eliseev A, Tsirlina G, Rubacheva A, Gañshina E, et al. *J Magn Magn Mater* 2009;321:833–5.
- [8] Song YY, Zhang D, Gao W, Xia XH. *Chem Eur J* 2005;11:2177–82.
- [9] Yu XD, Lee YJ, Furstenberg R, White JO, Braun PV. *Adv Mater* 2007;19:1689–92.
- [10] Napolskii KS, Sinitskii A, Grigoriev SV, Grigorieva NA, Eckerlebe H, Eliseev AA, et al. *Physica B* 2007;397:23–6.
- [11] Yan HW, Blanford CF, Lytle JC, Carter CB, Smyrl WH, Stein A. *Chem Mater* 2001;13:4314–21.
- [12] Freymann GV, John S, Schulz-Dobrick MT, Vekris EG, Tétreault NC, Wong S, et al. *Appl Phys Lett* 2004;84:224–6.
- [13] Luo Q, Liu ZJ, Li L, Xie SH, Kong JL, Zhao DY. *Adv Mater* 2001;13:286–9.
- [14] Sokolov S, Stein A. *Mater Lett* 2003;57:3593–7.
- [15] Li S, Zheng JT, Yang WY, Zhao YC. *Mater Lett* 2007;61:4784–6.
- [16] Hao YW, Zhu FQ, Chien CL, Searson PC. *J Electrochem Soc* 2007;154:D65–9.
- [17] Huang YJ, Lai CH, Wu PW. *Electrochem Solid-State Lett* 2008;12:20–2.
- [18] Reese CE, Asher SA. *J Colloid Interface Sci* 2002;248:41–6.
- [19] Eagleton TS, Searson PC. *Chem Mater* 2004;16:5027–32.
- [20] Chung YW, Leu IC, Lee JH, Yen JH, Hon MH. *J Electrochem Soc* 2007;6:E77–83.
- [21] Xia DY, Zhang JG, He X, Brueck SRJ. *Appl Phys Lett* 2008;93:071105.